

# TPSM Analysis of Structural Evolution in $^{109}\text{Sb}$

Aneeqa Basheer<sup>1</sup>, Ritvik Gupta<sup>1</sup>, Manvi Rajput<sup>1,\*</sup>, Suram Singh<sup>1,\*\*</sup>, G.H. Bhat<sup>2</sup>, and J.A. Sheikh<sup>3</sup>

<sup>1</sup>Department of Physics and Astronomical Sciences, Central University of Jammu, Samba, Jammu and Kashmir, (181143), India

<sup>2</sup>Government Degree College, Shopian, Jammu and Kashmir, (192303), India

<sup>3</sup>Department of Physics, Islamic University of Science and Technology, Awantipora, (192122), India

**Abstract.** The structural evolution of the odd-mass nucleus  $^{109}\text{Sb}$  has been investigated using the Triaxial Projected Shell Model (TPSM). This nucleus, located close to the  $Z = 50$  shell closure, serves as an ideal system for investigating the interplay between single-particle motion and collective rotation. Using angular-momentum projected quasiparticle configurations built on a triaxially deformed basis, we analyze the yrast and yrare band structures and compare the calculated energies with available experimental data. The TPSM results reproduce the observed band crossings and the overall evolution of the yrast and yrare bands reasonably well. A detailed examination of the dynamic moment of inertia,  $J^2$  and the reduced electric quadrupole transition probabilities reveals a gradual loss of collectivity with increasing spin for the yrast band, consistent with experimental observations. The present study provides a microscopic understanding of the structural evolution and decreasing collectivity in this nucleus.

## 1 Introduction

In atomic nuclei, angular momentum arises from both single-particle excitations and collective rotation. Depending on the nuclear mass, and deformation, the lowest-energy configurations at a given spin may be dominated either by collective rotational motion or by single-particle degrees of freedom in different nuclear regions ( $Z$ ,  $N$ ). Understanding this interplay is an important area of study, as it provides valuable insight into the underlying correlations of the nuclear many-body system [1].

Nuclei in the vicinity of  $A \sim 110$  region display a variety of collective rotational structures coexisting and competing with single-particle excitations along the angular momentum range. The rotational bands in this mass region arise from proton particle-hole excitations across the  $Z=50$  shell gap [2–5]. It has been observed with increasing rotational frequencies, the valence nucleons in these nuclei progressively align their angular-momentum vectors with the rotational axis, which leads to a decrease in dynamic moment of inertia with spin commonly termed as smooth band termination. The observed decrease in the  $J^2$ , associated with band termination, is a clear signature of the diminishing collective nature of the nuclear motion with increasing spin in this mass region.

\*e-mail: manvi.phy@cujammu.ac.in

\*\*e-mail: suram.phy@cujammu.ac.in

Collective structures in the Sn–Sb–Te mass region have been studied and a coexistence of single-particle states with collective structures has been identified [6]. In the  $Z=51$  Sb isotopes, collective bands are commonly interpreted as arising from a  $g_{9/2}$  proton hole coupled either to two-quasiparticle configurations or to  $2p-2h$  excitations of the Sn core. Consequently, the lighter Sb nuclei exhibit a variety of medium-spin structures dominated by  $h_{11/2}$  particle and  $g_{9/2}$  hole configurations [7, 8]. Transfer-reaction studies on light Sb isotopes suggest that the lowest-lying states are largely single-particle in nature, while certain low-spin positive-parity states exhibit weaker collectivity and are often interpreted as arising from coupling to low-lying core excitations of the Sn nucleus [9]. While such observations clearly establish a distinction between single-particle and collective structures for the positive-parity states, particularly with increasing spin, the corresponding evolution of the negative-parity states in odd-mass Sb nuclei have not been investigated with comparable clarity.

As one moves towards the lighter end of the Sb isotopic chain,  $^{109}\text{Sb}$  emerges as a particularly interesting case for examining the evolution of collectivity with increasing spin. Several experimental investigations have revealed compelling evidence for a gradual loss of collectivity with increasing rotational frequency. Intruder rotational bands have been traced to very high frequencies, with five decoupled bands. The  $J^2$  values for four of these bands is seen to decrease to unusually low values at higher frequencies, indicating a pronounced reduction of collective rotational motion [10]. Complementary, lifetime measurements for the terminating band in  $^{109}\text{Sb}$  further support this interpretation by demonstrating a systematic decrease in  $B(E2)$  transition strengths with spin, providing direct evidence for the weakening of collectivity towards band termination [11]. The coexistence of different states, the onset of band termination, and the pronounced structural sensitivity makes this isotope an ideal testing ground for microscopic models. Motivated by the absence of a comprehensive theoretical description of its structural evolution, we investigate  $^{109}\text{Sb}$  using the framework of Triaxial Projected Shell Model (TPSM) [12].

The article is structured as follows: the theoretical framework is introduced in the next section, the results obtained from the calculations are discussed subsequently, and the main conclusions are presented in the last section.

## 2 Theoretical Framework

The theoretical framework employed in the current study is the TPSM, a microscopic method that extends the conventional shell-model description by incorporating nuclear deformation in a self-consistent manner. The single-particle basis is obtained from a triaxial Nilsson mean-field by adopting optimum quadrupole deformation parameters,  $\epsilon$  and  $\epsilon'$ . While the formalism allows for arbitrary choices of deformation, the use of optimal values appropriate to the nucleus under study ensures a reliable description of the Fermi surface. This, in turn, permits a truncated yet sufficient configuration space focused on states near the Fermi level. The theoretical framework has been extensively discussed in previous publications [12–16]. Therefore, only a concise outline of the formalism and the key equations employed in the present calculations is provided here.

The intrinsic states generated in a deformed basis lack good angular momentum due to the broken rotational symmetry. This symmetry is restored by applying the three-dimensional angular-momentum projection operator, expressed as

$$\hat{P}_{MK}^I = \frac{2I+1}{8\pi^2} \int d\Omega D_{MK}^I(\Omega) \hat{R}(\Omega), \quad (1)$$

In the current work, the projected basis is comprised of one-proton and one-proton plus two-neutron configurations, i.e.,

$$\{\hat{P}_{MK}^I a_{p_1}^\dagger |\Phi\rangle, P_{MK}^I a_{p_1}^\dagger a_{n_1}^\dagger a_{n_2}^\dagger |\Phi\rangle\}, \quad (2)$$

The Hamiltonian used in this formalism is given below:

$$\hat{H} = \hat{H}_0 - \frac{1}{2}\chi \sum_{\mu} \hat{Q}_{\mu}^{\dagger} \hat{Q}_{\mu} - G_M \hat{P}^{\dagger} \hat{P} - G_Q \sum_{\mu} \hat{P}_{\mu}^{\dagger} \hat{P}_{\mu}. \quad (3)$$

where,  $\hat{H}_0$  represents the spherical harmonic-oscillator single particle hamiltonian. The diagonalization of Hamiltonian using the projected basis is done in the final step of the calculation.

The  $G_M$  in the equation 3 represents the monopole pairing strength given by:

$$G_M = (G_1 \mp G_2 \frac{N-Z}{A}) \frac{1}{A} (MeV), \quad (4)$$

where the negative or positive sign is applied to neutrons or protons respectively.  $G_1$  and  $G_2$  are chosen to account for measured mass discrepancies and hence depend on the mass region under consideration. In the current calculations the values  $G_1 = 20.70$  and  $G_2 = 12.12$  are employed. The adopted value of  $G_M$  is well suited to the chosen single-particle model space, which includes three major shells for each type of nucleon. For the present calculations  $N = 3, 4, 5$  have been used for both protons and neutrons.

In addition, the TPSM framework incorporates two essential deformation parameters,  $\epsilon$  and  $\epsilon'$ , which describe the axial and non-axial components of the nuclear shape, respectively. In the current analysis, the values  $\epsilon = 0.250$  and  $\epsilon' = 0.108$  are adopted. The presence of prolate deformation in this isotope has been already discussed in the literature, for example in the works of Ishii et al. [17] and Wadsworth et al. [11]. The value of  $\epsilon'$  is chosen such that the bandhead of yrare band is reproduced [18].

## 3 Results and Discussion

### 3.1 Band Diagrams

The projected energies obtained from the one-quasiparticle (1-qp) and three-quasiparticle (3-qp) configurations, calculated using the deformation parameters specified in Sec. 2, are shown in Fig. 1 for  $^{109}\text{Sb}$ . Such plots are referred to as band diagrams in the projected shell model (PSM) framework [19]. Band diagrams display the angular-momentum projected energies of intrinsic configurations prior to configuration mixing and are particularly useful for identifying band crossings and associated structural changes in the calculated spectra. These diagrams are quite significant as they provide direct insight into the underlying structure of the yrast states.

In this figure, we have depicted four bands in total, two of these are 1-qp bands with quasiparticle energies 1.435 MeV and 2.435 MeV respectively and the other two are 3-qp bands with energies 5.198 MeV and 4.610 MeV respectively. In TPSM, the use of a triaxial basis implies that the intrinsic states are not characterized by a definite  $K$ . Consequently, each configuration appearing in Eq. 2 contains contributions from multiple  $K$  components. The band structures displayed in the band diagrams are generated by selecting a particular  $K$  value through the angular-momentum projection procedure. In this particular calculation, 1-qp bands are based on  $K = 3/2, 7/2$  and  $11/2$  configurations whereas the 3-qp bands are based on  $K = 1/2, 5/2$  and  $9/2$  configurations respectively.

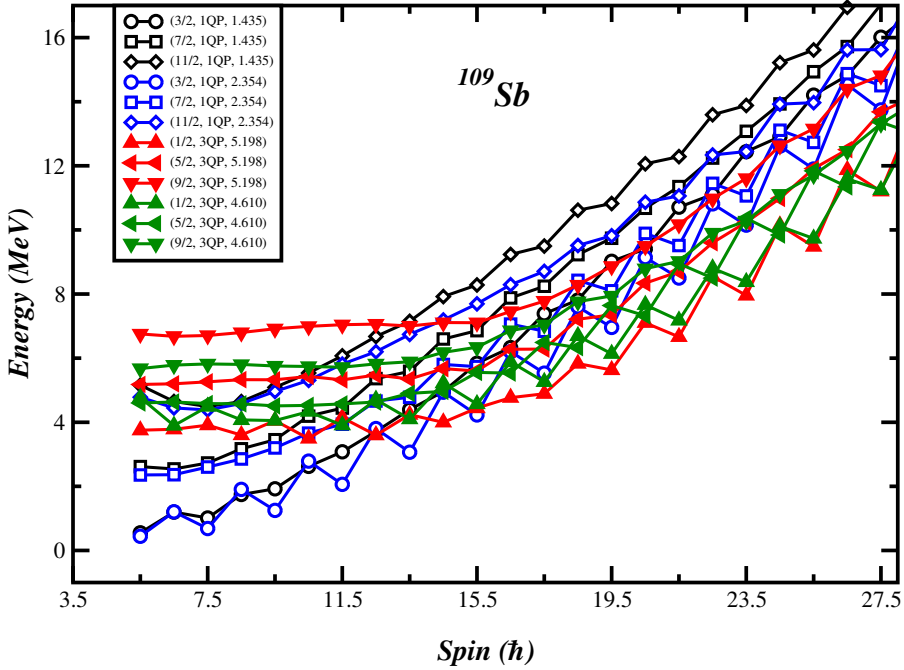


**Figure 1.** Band diagram for  $^{109}\text{Sb}$  using TPSM. The legends in the figure are of the form (K, Str, Eqp) where K denotes the K quantum number, Str. depicts the structure of the band i.e., 1QP which indicates  $1\pi$  configuration here or 3QP which indicates  $1\pi 2\nu$  configuration and Eqp denotes the quasiparticle energy.

The structure of the yrast band can be interpreted from Fig. 1. At lower spins, the yrast band is comprised by 1-qp band with  $K=3/2$  and a quasiparticle energy of 2.354 MeV. The energies of the 3-qp bands decrease gradually as spin increases, and at around  $I = 33/2^-$ , a 3-qp band with quasiparticle energy 5.198 MeV and  $K=1/2$  crosses the 1-qp band and subsequently becomes yrast. At higher spins another 3-qp band competes with the previously lowest 3-qp band to form the yrast. This clearly indicates a crossing between the 1-qp and 3-qp configurations. Such a crossing can be attributed to the breaking of a neutron pair with increasing angular momentum, leading to a change in the underlying quasiparticle configuration.

### 3.2 Projected Energies

To investigate the microscopic origin of the yrast and yrare bands, angular-momentum projection is performed on the intrinsic quasiparticle configurations as discussed in section 2. The projected energies, obtained after diagonalization of the Hamiltonian and configuration mixing are evaluated as a function of spin.

Experimentally, the first study reporting the negative-parity yrast band in  $^{109}\text{Sb}$  was carried out by Janzen and collaborators [20]. In that work, three rotational bands were identified.

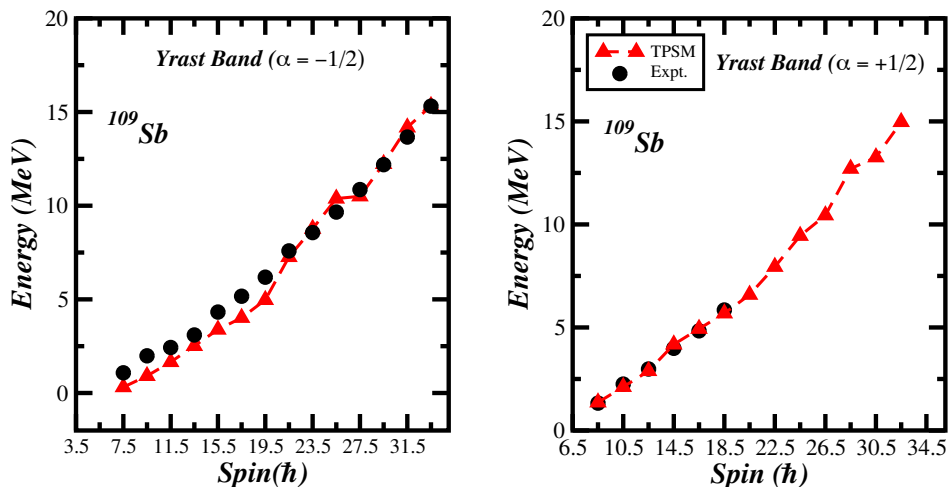


**Figure 2.** Comparison of TPSM yrast energies with experimental yrast energies [10] for  $^{109}\text{Sb}$ .

The yrast band was interpreted as arising from a proton occupying the  $h_{11/2}$  orbital coupled to a deformed  $^{108}\text{Sn}$  core with a quadrupole deformation of  $\beta = 0.2$ . Subsequently, additional bands in  $^{109}\text{Sb}$  were investigated by Schnare et al. [10], where smooth band termination was noticed in many intruder configurations.

Figure 2 presents a comparison between the calculated yrast-band energies for  $^{109}\text{Sb}$  and the available experimental data. The left panel corresponds to the  $\alpha = -1/2$  signature, while the right panel shows the  $\alpha = +1/2$  signature. Overall, the theoretical results show good agreement with the experimental data. However, a closer inspection reveals that for low to medium spins, up to  $I = 39/2^-$ , the agreement is relatively poorer compared to that at higher spins. The precise reason behind this must be the proximity of  $^{109}\text{Sb}$  to the closed-shell configuration, where the low-lying states are expected to retain a more pronounced spherical character. If this is indeed the case, it suggests the possible coexistence of single-particle and collective structures in this isotope. To examine this possibility, we have performed TPSM calculations for the low-lying states of  $^{109}\text{Sb}$  using a significantly reduced deformation parameter,  $\epsilon = 0.093$ , and compared the resulting energies with the corresponding experimental data, as shown in Fig. 3. A pronounced difference is observed between the energies obtained using the low deformation and those calculated with the optimum deformation. Notably, the results obtained with the smaller deformation reproduce the experimental low-spin energies more accurately, supporting the interpretation of a predominantly spherical or weakly deformed character for the low-lying states. A shell-model study of the low-lying states in  $^{109}\text{Sb}$  has

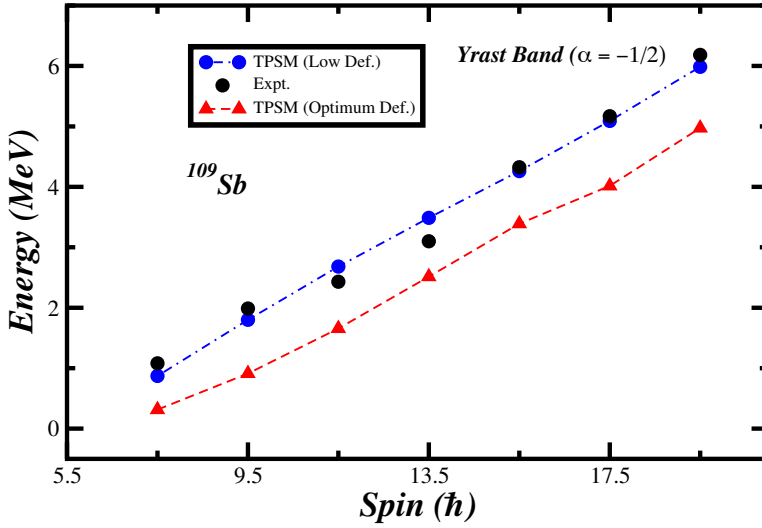


**Figure 3.** Comparison of TPSM yrast energies obtained using low and optimum deformation parameters with experimental energies [10] for  $^{109}\text{Sb}$ .

also been reported, which supports our interpretation of a weakly deformed character at low spins, although that work was limited to positive-parity states. Furthermore, The TPSM results for the yrare bands show excellent consistency with the experimental energies over the full spin range, as shown in Fig. 4.

### 3.3 Decreasing Collectivity in $^{109}\text{Sb}$

At high angular momentum, rotational bands in nuclei often exhibit a gradual loss of collectivity as the spin vectors of the valence quasiparticles align along the rotational axis. This phenomenon, commonly referred to as decreasing collectivity, is a characteristic feature of smoothly terminating bands and has been reported extensively in nuclei with mass numbers around  $A \sim 110$ . In order to investigate the evolution of collectivity in  $^{109}\text{Sb}$ , we examine two key observables that are particularly responsive to any changes in nuclear structure at high spin:  $J^2$ , the dynamic moment of inertia, and  $B(E2)$ , the reduced electric quadrupole transition probabilities. Together, these quantities provide complementary information on the rotational response and the degree of quadrupole collectivity as the band approaches termination.

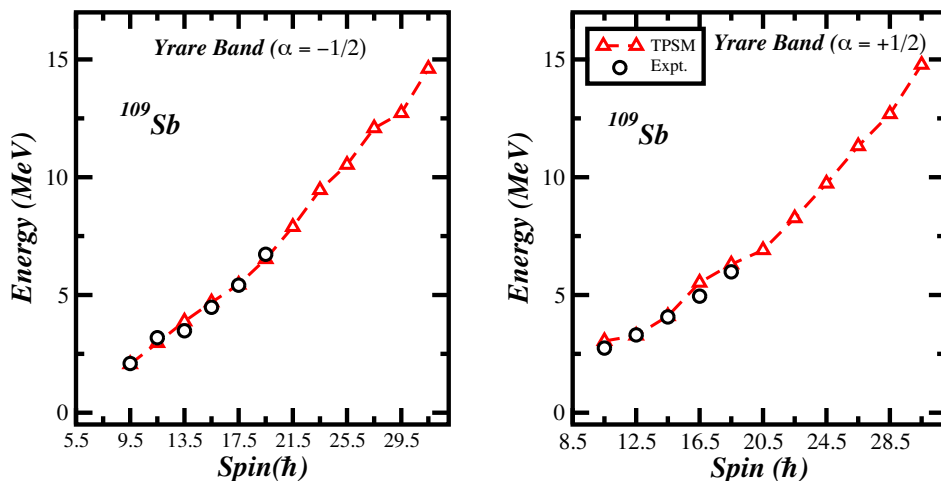


**Figure 4.** Comparison of TPSM yrare energies with experimental yrare energies [10] for  $^{109}\text{Sb}$ .

### 3.3.1 Dynamic Moment of Inertia

One of the most important quantities characterizing a nuclear rotational band is the moment of inertia. The dynamic moment of inertia plays a crucial role in the analysis of high-spin rotational bands, as analyzing its behaviour is quite helpful to track any changes in the underlying nuclear structure. The dynamic moment of inertia is obtained from the slope of the angular momentum as a function of rotational frequency,  $J^2 = dI/d\omega$ , and this quantity provides a direct measure of the incremental response of the nucleus to rotation. As a result,  $J^2$  is an effective probe of alignment processes, band crossings, and the gradual loss of collectivity at high rotational frequencies.

Experimentally, the yrast intruder band in  $^{109}\text{Sb}$  exhibits a pronounced decrease in the  $J^2$  as rotational frequency increases. In the pioneering work of Janzen et al. [20], the extracted  $J^2$  values were found to decrease smoothly with increasing frequency, eventually attaining unusually low values. Subsequent high-spin measurements by Schnare et al. [10] confirmed this behaviour and demonstrated that the gradual reduction of  $J^2$  persists up to the highest observed spins, with no abrupt band crossings at high frequency. This smooth and systematic decline of the dynamic moment of inertia provides compelling experimental evidence for the progressive loss of collectivity in the yrast band of  $^{109}\text{Sb}$ .

The  $J^2$  for the yrast band of  $^{109}\text{Sb}$  exhibits characteristic features that reflect the underlying structural evolution with spin as can be seen in Fig. 5. At low spins, the  $J^2$  values remain relatively small, indicating a predominantly single-particle character of the yrast states and,

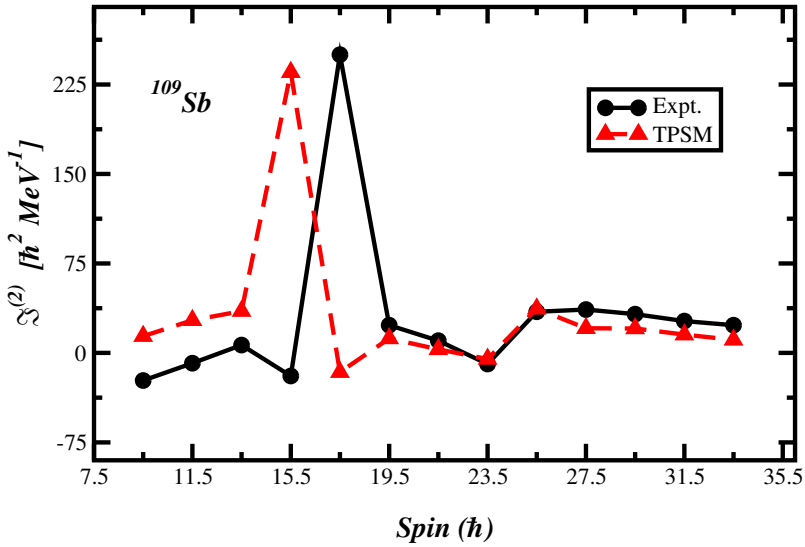


**Figure 5.** Comparison of TPSM and experimental  $J^2$  values [10] for yrast band of  $^{109}\text{Sb}$ .

consequently, a reduced degree of collectivity. With increasing angular momentum, a pronounced peak in  $J^2$  is observed around  $I = 33/2^-$ , which can be attributed to a band crossing between competing quasiparticle configurations. Such a crossing leads to rapid changes in the level spacings and is therefore strongly manifested in the dynamic moment of inertia. Beyond this crossing region, the yrast band settles into a well-defined rotational structure; however, as the spin increases further,  $J^2$  begins to decrease smoothly. This gradual reduction at higher spins reflects loss of quadrupole collectivity, signaling the onset of smooth band termination. The overall behavior of  $J^2$ , including its mid-spin rise due to band crossing, and high-spin decline, is consistently reproduced by the TPSM calculations.

### 3.3.2 Reduced Transition Probability

The reduced electric quadrupole transition probabilities  $B(E2)$  provide a direct measure of quadrupole collectivity in rotational bands. Their evolution with spin is particularly sensitive to changes in nuclear deformation and the gradual loss of collectivity at high angular momentum.

The behavior of the  $B(E2)$  values along the yrast band of  $^{109}\text{Sb}$  offers a clear picture of how collectivity evolves with spin as can be seen in Fig. 6. At low spins, the  $B(E2)$  strengths are increasing with spin depicting a structural evolution from single-particle motion towards weak collectivity. As the spin increases, the  $B(E2)$  values rise and reach moderate

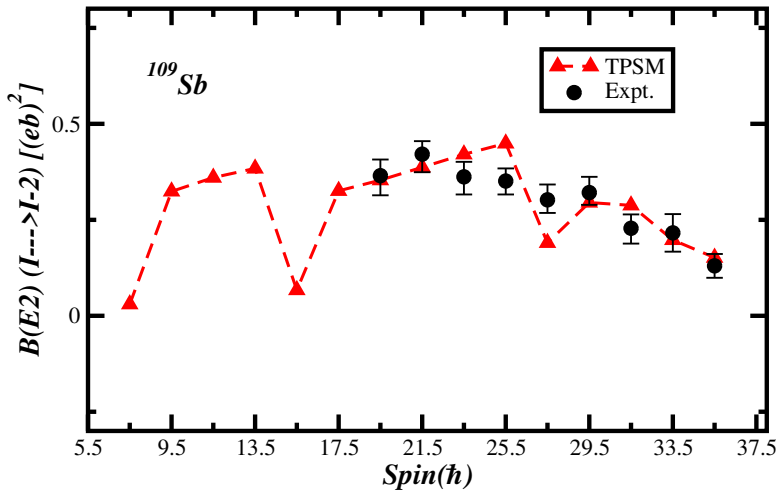


**Figure 6.** Comparison of TPSM and experimental BE(2) values [11] for yrast band of  $^{109}\text{Sb}$ .

strengths, suggesting the development of collective rotational motion. A noticeable dip in the B(E2) values is observed, which signals a structural change associated with a band crossing in this spin region. Beyond this crossing, the B(E2) strengths recover briefly before beginning to decrease steadily at higher spins. This subsequent reduction reflects the gradual loss of quadrupole collectivity. A similar trend has been observed experimentally from lifetime measurements in  $^{109}\text{Sb}$  [11], where the BE(2) values were found to decrease smoothly with increasing spin, providing strong evidence for smooth band termination. The close match between the TPSM results and the experimental data therefore reinforces the interpretation that the high-spin yrast states in  $^{109}\text{Sb}$  evolve from a weakly collective regime into a non-collective terminating structure.

## 4 Summary

In this work, the high-spin structure of the odd-mass nucleus  $^{109}\text{Sb}$  has been studied using the TPSM. The yrast and yrare band structures were analyzed through band diagrams and projected energies. The calculated results successfully reproduce the key features of the experimental spectra, including the observed band crossings and the overall spin dependence of the yrast and yrare bands.

A detailed investigation of the dynamic moment of inertia  $J^2$  shows characteristic behavior associated with the evolution of nuclear structure. At low spins, the relatively small

$J^2$  values indicate a dominant single-particle character. A pronounced enhancement of  $J^2$  at intermediate spins is attributed to a band crossing between competing quasiparticle configurations, while the smooth decrease at higher spins reflects the gradual loss of collectivity and the onset of smooth band termination. The evolution of the reduced electric quadrupole transition probabilities  $B(E2)$  further supports this interpretation, with decreasing  $B(E2)$  strengths at higher spins signaling a reduction in quadrupole collectivity as the terminating states are approached.

Overall, the present TPSM analysis provides a consistent microscopic description of the coexistence of single-particle and collective structures in  $^{109}\text{Sb}$  and offers a unified interpretation of the experimentally observed decreasing collectivity in this nucleus.

## Acknowledgement

A.B. gratefully acknowledges financial support from the Department of Science and Technology, Government of India, under the DST–INSPIRE Fellowship (Sanction No. DST/INSPIRE Fellowship/2021/IF210230). S. Singh acknowledges support from the Science and Engineering Research Board (SERB), Department of Science and Technology, Government of India, through Grant No. CRG/2022/002384.

## References

- [1] A. V. Afanasjev, D. B. Fossan, G. J. Lane, and I. Ragnarsson, Termination of rotational bands: Disappearance of quantum many-body collectivity. *Phys Reports* **322**, 1-124 (1999). <https://doi.org/10.1016/S0370-1573>
- [2] W. Dietrich et al., Possible rotational states in odd In nuclei. *Nucl Phys A* **253**, 429-44 (1975). [https://doi.org/10.1016/0375-9474\(75\)90490-X](https://doi.org/10.1016/0375-9474(75)90490-X)
- [3] A. K. Gaigalas, R. E. Shroy, G. Schatz, and D. B. Fossan, Deformed  $9/2^+$  States and  $\Delta J=1$  Rotational Bands in  $^{113,115,117,119}\text{Sb}$  Nuclei. *Phys Rev Letts* **35**, 555-558 (1975). <https://doi.org/10.1103/PhysRevLett.35.555>
- [4] D. B. Fossan et al, Deformed  $9/2^+$  proton-hole states in odd-A I nuclei. *Phys Rev C* **15**, 1732–1746 (1977). <https://doi.org/10.1103/PhysRevC.15.1732>
- [5] J. Bron et al, Collective bands in even mass Sn isotopes. *Nucl Phys A* **318**, 335–356 (1979). [https://doi.org/10.1016/0375-9474\(79\)90653-5](https://doi.org/10.1016/0375-9474(79)90653-5)
- [6] J. J. Ressler et al, First observation of  $^{109}\text{Te}$   $\beta^+$  and electron-capture decay to levels of  $^{109}\text{Sb}$ . *Phys Rev C* **66**, 024308 (2002). <https://doi.org/10.1103/PhysRevC.66.024308>
- [7] R. E. Shroy, A. K. Gaigalas, G. Schatz, and D. B. Fossan, High spin states in odd-mass  $^{113-119}\text{Sb}$ :  $\Delta J = 1$  bands on  $9/2^+$  proton states. *Phys Rev C* **19**, 1324-1331 (1979). <https://doi.org/10.1103/PhysRevC.19.1324>
- [8] V. P. Janzen et al, The proton  $h_{11/2}$  intruder orbital: Evidence for collectivity and a strong proton-neutron interaction. *Phys Rev Letts* **70**, 1065-1068 (1993). <https://doi.org/10.1103/PhysRevLett.70.1065>
- [9] R. Kammermans, T. J. Ketel, and H. Verheul, Excited states of odd-A Sb isotopes  $^{115,113,111}\text{Sb}$ . *Zeits for Phys A* **279**, 99-103 (1976). <https://doi.org/10.1007/BF01409096>
- [10] H. Schnare et al, Smooth termination of intruder bands in  $^{109}\text{Sb}$ . *Phys Rev C* **54**, 1598-1609 (1996). <https://doi.org/10.1103/PhysRevC.54.1598>
- [11] R. Wadsworth et al, Decreasing collectivity in smoothly terminating bands in the  $A \sim 110$  region. *Phys Rev Letts* **80**, 1174 (1998). <https://doi.org/10.1103/PhysRevLett.80.1174>
- [12] J. A. Sheikh and K. Hara, Triaxial projected shell model. *Phys Rev Letts* **82**, 3968-3971 (1999). <https://doi.org/10.1103/PhysRevLett.82.3968>

- [13] J. A. Sheikh et al, Triaxial projected shell model study of  $\gamma$ -vibrational bands in even-even Er isotopes. *Physical Review C* **77**, 034313 (2008). <https://doi.org/10.1103/PhysRevC.77.034313>
- [14] A. Basheer et al, Insights into triaxial collectivity of odd-mass  $^{111-119}\text{Sb}$  isotopes. *Nuclear Physics A* **1067**, 123299 (2026). <https://doi.org/10.1016/j.nuclphysa.2025.123299>
- [15] M. Sharma et al, Shape evolution of even-even strontium isotopes near the  $N = 50$  shell closure. *The European Physical Journal A* **61**, 113 (2025). <https://doi.org/10.1140/epja/s10050-025-01585-7>
- [16] M. Rajput et al, Triaxial projected shell model study of  $\gamma$ -bands in even-even  $^{104-122}\text{Cd}$  nuclei. *Nuclear Physics A* **1019**, 122383 (2022). <https://doi.org/10.1016/j.nuclphysa.2022.122383>
- [17] T. Ishii, A. Makishima, M. Shibata, M. Ogawa, and M. Ishii, Nuclear structure of  $^{109}\text{Sb}$ . *Phys Rev C* **49**, 2982-2989 (1994). <https://doi.org/10.1103/PhysRevC.49.2982>
- [18] J. A. Sheikh et al, Multi-phonon  $\gamma$ -vibrational bands in odd-mass nuclei studied by triaxial projected shell model approach. *Phys Letts B* **688**, 305-308 (2010). <https://doi.org/10.1016/j.physletb.2010.04.027>
- [19] K. Hara and Y. Sun, Projected shell model and high-spin spectroscopy. *Int J of Modern Phys E* **4**, 637-785 (1995). <https://doi.org/10.1142/S0218301395000250>
- [20] V. P. Janzen et al, New features of collective nuclear rotation at very high frequency in  $^{109}\text{Sb}$ . *Phys Rev Letts* **72**, 1160-1163 (1994). <https://doi.org/10.1103/PhysRevLett.72.1160>